

Article

Evaluation of Airborne Lidar Elevation Surfaces for Propagation of Coastal Inundation: The Importance of Hydrologic Connectivity

Sandra Poppenga ^{1,†,*} and Bruce Worstell ^{2,†}

¹ U.S. Geological Survey, Earth Resources Observation and Science (EROS) Center, Sioux Falls 57198, SD, USA

² Stinger Ghaffarian Technologies Inc., Contractor to the U.S. Geological Survey, Earth Resources Observation and Science (EROS) Center, Sioux Falls, SD 57198, USA; E-Mail: worstell@usgs.gov

† These authors contributed equally to this work.

* Author to whom correspondence should be addressed; E-Mail: spoppenga@usgs.gov; Tel.: +1-605-594-2634 (ext. 2634); Fax: +1-605-594-6529.

Academic Editors: Guy J-P. Schumann, Magaly Koch and Prasad S. Thenkabail

Received: 12 June 2015 / Accepted: 8 September 2015 / Published: 14 September 2015

Abstract: Detailed information about coastal inundation is vital to understanding dynamic and populated areas that are impacted by storm surge and flooding. To understand these natural hazard risks, lidar elevation surfaces are frequently used to model inundation in coastal areas. A single-value surface method is sometimes used to inundate areas in lidar elevation surfaces that are below a specified elevation value. However, such an approach does not take into consideration hydrologic connectivity between elevation grids cells resulting in inland areas that should be hydrologically connected to the ocean, but are not. Because inland areas that should drain to the ocean are hydrologically disconnected by raised features in a lidar elevation surface, simply raising the water level to propagate coastal inundation will lead to inundation uncertainties. We took advantage of this problem to identify hydrologically disconnected inland areas to point out that they should be considered for coastal inundation, and that a lidar-based hydrologic surface should be developed with hydrologic connectivity prior to inundation analysis. The process of achieving hydrologic connectivity with hydrologic-enforcement is not new, however, the application of hydrologically-enforced lidar elevation surfaces for improved coastal inundation mapping as approached in this research is innovative. In this article, we propagated a

high-resolution lidar elevation surface in coastal Staten Island, New York to demonstrate that inland areas lacking hydrologic connectivity to the ocean could potentially be included in inundation delineations. For inland areas that were hydrologically disconnected, we evaluated if drainage to the ocean was evident, and calculated an area exceeding 11 ha (~0.11 km²) that could be considered in inundation delineations. We also assessed land cover for each inland area to determine the type of physical surfaces that would be potentially impacted if the inland areas were considered as part of a coastal inundation. A visual analysis indicated that developed, medium intensity and palustrine forested wetland land cover types would be impacted for those locations. This article demonstrates that hydrologic connectivity is an important factor to consider when inundating a lidar elevation surface. This information is needed for inundation monitoring and management in sensitive coastal regions.

Keywords: hydrologic connectivity; coastal inundation delineation; lidar; propagation

1. Introduction/Background

Hazardous coastal inundation is escalating in vulnerable ecosystems [1,2] resulting in the need to accurately predict inundation in coastal areas that are impacted by natural disasters [3,4–6]. Detailed light detection and ranging (lidar) elevation surfaces are important for understanding the likely impacts and vulnerability of coastal inundation from storm surge, flooding events, and sea-level rise [3,7–10]. Therefore, Federal and State agencies are increasingly relying on lidar remote sensing technology for delineating inundation zones and developing guidelines for flood risk zone estimates [11]. Planners and water resource managers responsible for mitigating associated risks and costs to communities and ecosystems also rely on elevation-based predictions for coastal inundation mapping. Thus, lidar elevation surfaces are critical for modeling the volume of water flow over the topography to determine elevations at risk from coastal inundation [12–17]. The accuracy of coastal inundation predictions, however, is dependent upon inundation methods that account for hydrologic connectivity of inland and ocean waters in a highly detailed lidar elevation surface [12–15].

Hydrologic connectivity is achieved with hydrologic (hydro)-enforcement, which simulates overland surface flow in a lidar-based digital elevation model (DEM) in locations that become impounded by elevated features (bridges/roads) that would flood in a given event [9,10,12]. Despite the high-resolution and high-vertical accuracy of lidar elevation surfaces, the detailed topography presents challenges for identifying inundated elevations [9,10,12,13]. A common problem encountered in lidar DEM hydrological modeling is the presence of elevated structures, such as bridges or roads overlying underground drainage structures (culverts) [9,10,12,13,18,19].

Diaz-Nieto *et al.* addressed this hydrologic connectivity issue by using a water balance approach to develop a screening tool for flood risk area identification. They stated this approach would avoid the complexities of overland flow modeling in an urban environment [18]; however, they used a combination of water features greater than 1 m wide and Google Earth images to determine likely flow paths surrounding elevated (bridge) structures, and assumed that all depressions in the lidar DEM were genuine [18]. Hydrologic connectivity between upstream and downstream areas surrounding culvert locations was not

directly addressed. Abdullah *et al.* [19] employed lidar point cloud filtering techniques to develop digital terrain models (DTMs) for urban flood modeling. Their methodology was comprised of data fusion combined with an analysis of lidar intensity, height, and slope. Rather than using automated methods to identify elevated structures, they overlaid vector river polygons on the lidar point cloud data. They noted that the use of DTMs for flood modeling applications cannot always be considered suitable depending on the terrain characteristics [19].

Poulter and Halpin [20] modeled sea-level rise with various approaches ranging from the “bathtub fill” (single-value surface method) to inundating lands that are hydrologically connected to the ocean, thereby forcing coastal inundation to occur only where low-lying elevations are hydrologically connected to the ocean [8,20–22]. Poulter and Halpin [20] stated that inundating lidar elevation data is sensitive to horizontal resolution and the modeling of hydrological connectivity. However, they noted that hydrologic connectivity resulted in inundation that closely followed the enforced drainage network for a hydro-corrected DEM. They also indicated that the “bathtub” method does not consider surface hydrologic connectivity between grid cells and can create erroneous inundated areas that are not connected to the ocean [20,21].

Therefore, because inland areas that should drain to the ocean are hydrologically disconnected by raised features in a lidar elevation surface, simply raising the water level (“bathtub fill”) to propagate coastal inundation will lead to inundation uncertainties. We took advantage of this issue to identify hydrologically disconnected inland areas, and to point out that they should be considered for coastal inundation. The objective of this article is to propagate coastal inundation in a lidar elevation surface to identify inland areas that are not hydrologically connected to the ocean. These inland areas can become excluded from inundation delineations in a high-resolution, high-accuracy elevation surface because they are not hydrologically connected to ocean waters. The process of achieving hydrologic connectivity in a lidar DEM with hydro-enforcement is not new [9,10,12,13,18], however, the application of hydro-enforced lidar elevation surfaces for improved coastal inundation mapping as approached in this research is innovative. Hydrologically-connected lidar elevation surfaces are not always considered in hydrologic analyses, therefore, we evaluated propagated coastal inundation in the southern part of Staten Island, New York; a coastal ecosystem that was severely impacted by Hurricane Sandy in 2012 [23]. We also assessed the land cover type for each inland area to determine the physical surfaces that would be potentially impacted should the inland areas be considered as part of a coastal inundation. This work demonstrates that an analysis of hydrologic information derived from remotely sensed lidar elevation surfaces is needed for coastal inundation monitoring and management in sensitive coastal areas that are at risk for natural disasters.

2. Study Area

The study area is located in the southern part of Staten Island, New York, one of five boroughs of New York City (Figure 1). In the study area, surface waters radiate from higher elevations and flow generally toward the coast discharging into the Atlantic Ocean. Staten Island drains an elevation-derived area of 183.3 km² with a minimum elevation at the coast and a maximum elevation value of 125.6 m. The landscape in the study area consists of developed areas interspersed with forest land, including tidal wetlands and water. This densely populated area was part of a second-ever mandatory evacuation

according to New York City Office of Emergency Management [24] and was severely impacted by Hurricane Sandy when it made landfall on 30 October 2012 [23].

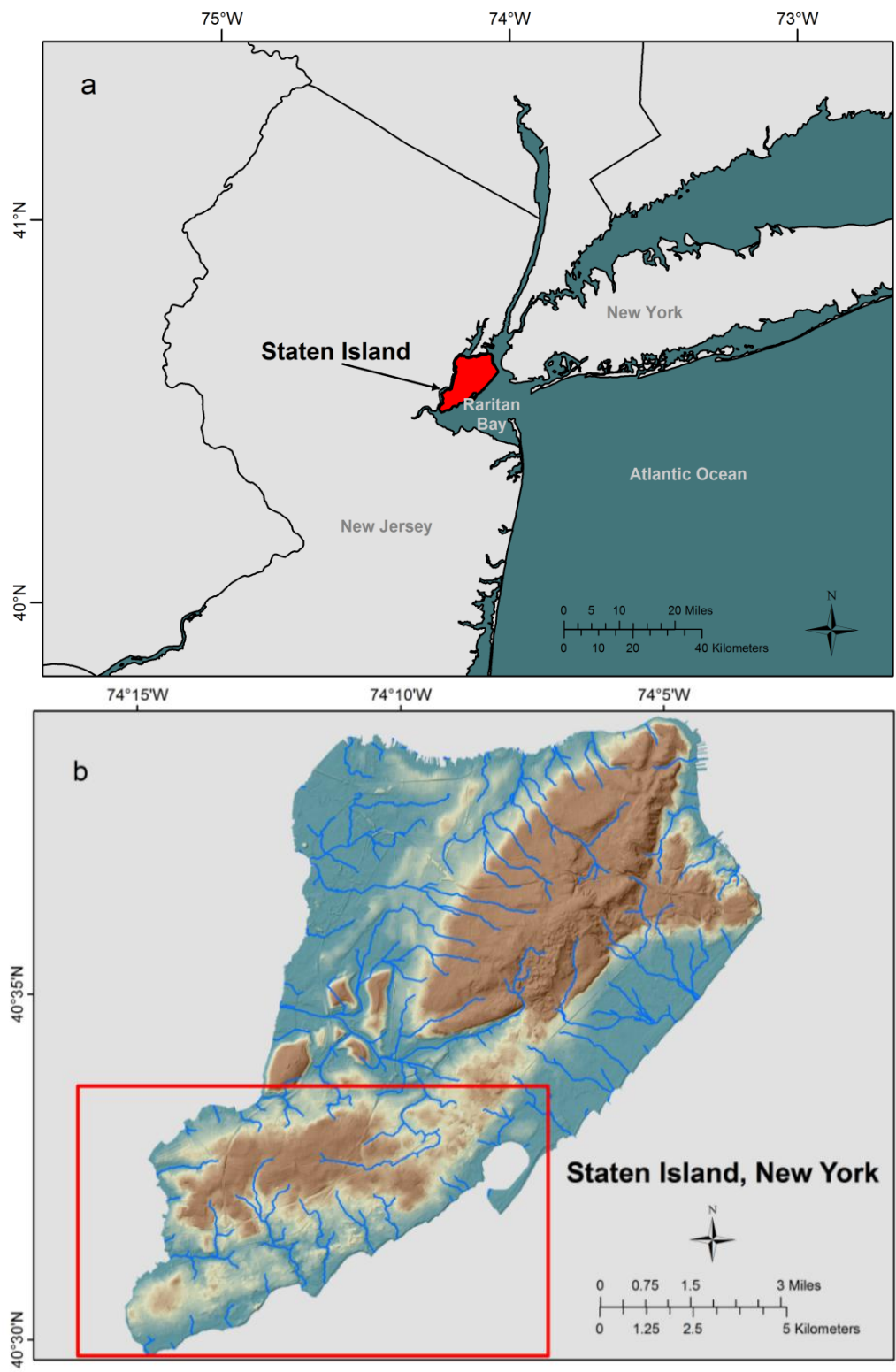


Figure 1. Study area of Staten Island, New York. (a) shows the location of Staten Island, New York. (b) shows the study area of Staten Island, New York.

3. Methods

3.1. Data and Pre-Processing

Remotely sensed airborne lidar point cloud data were acquired over Richmond County, New York by Woolpert [25]. The lidar collection was acquired from 5 August 2013 to 15 August 2013 as part of ten missions flown over the greater New York City at 0.7 m nominal post spacing using a Leica ALS70 500 kHz lidar system on board a Cessna 402. The flight lines were flown at an average of 2286 m above ground level [25,26].

The high-resolution (1 m) lidar elevation grid, provided by the vendor [25], was transformed to Universal Transverse Mercator Zone 18, North American Datum 1983 in units of meters. The vertical datum was the North American Vertical Datum of 1988 (NAVD88) in units of meters. As reported by the vendor, the bare earth DEM fundamental vertical accuracy tested 12.1 cm at the 95-percent confidence level on open bare earth terrain. Vertical accuracy was not reported by the vendor on vegetated areas. The vendor-provided lidar elevation surface was used to propagate flood waters in Staten Island, New York.

3.2. Propagation of Flood Waters in a Lidar Elevation Surface

To demonstrate that raising elevation values in elevation surfaces does not account for hydrologic connectivity between inland and ocean waters, we used the single-value surface method as a tool to inundate the high-resolution (1 m) lidar elevation surface. This process, often called a bathtub technique, has two variables: the inundation level and the ground elevation [20,22]. We identified an inundation level and applied it to the (1 m) lidar elevation surface in the study area to show the importance of hydrologic connectivity in an inundation analysis. It should be noted that we used the single-value surface method as a tool rather than a more complex hydrologic model; we used this tool to demonstrate that inland areas in the lidar elevation surface that were hydrologically disconnected to the ocean could be potentially included in inundation delineations.

In the aftermath of Hurricane Sandy, high-water marks (HWMs) were surveyed relative to NAVD88 by the U.S. Geological Survey (USGS) in cooperation with the Federal Emergency Management Agency (FEMA) with particular emphasis in New York and New Jersey where the impacts of the storm were the most pronounced [27,28]. HWMs were surveyed to a vertical accuracy of 0.26 ft (0.079 m) at the 95-percent confidence level and within 10 ft (3.048 m) horizontally [27]. In the study area, we used the USGS HWMs to derive an inundation value to apply to the lidar elevation surface.

Based upon an elevation mean of the USGS HWMs in the study area (Figure 2), we identified an inundation level of 4.51 m (Table 1). Using ArcGIS Spatial Analyst Raster Calculator, we set the inundation level at 4.51 m in the lidar elevation surface. In this example, all grid cells less than or equal to 4.51 m represented inundated elevations in the lidar elevation surface; grid cells greater than the specified 4.51 m represented elevations that were not inundated in this example and were removed from the selection; thereby generating a delineation of projected inundation areas using ArcGIS Spatial Analyst Region Group tool.

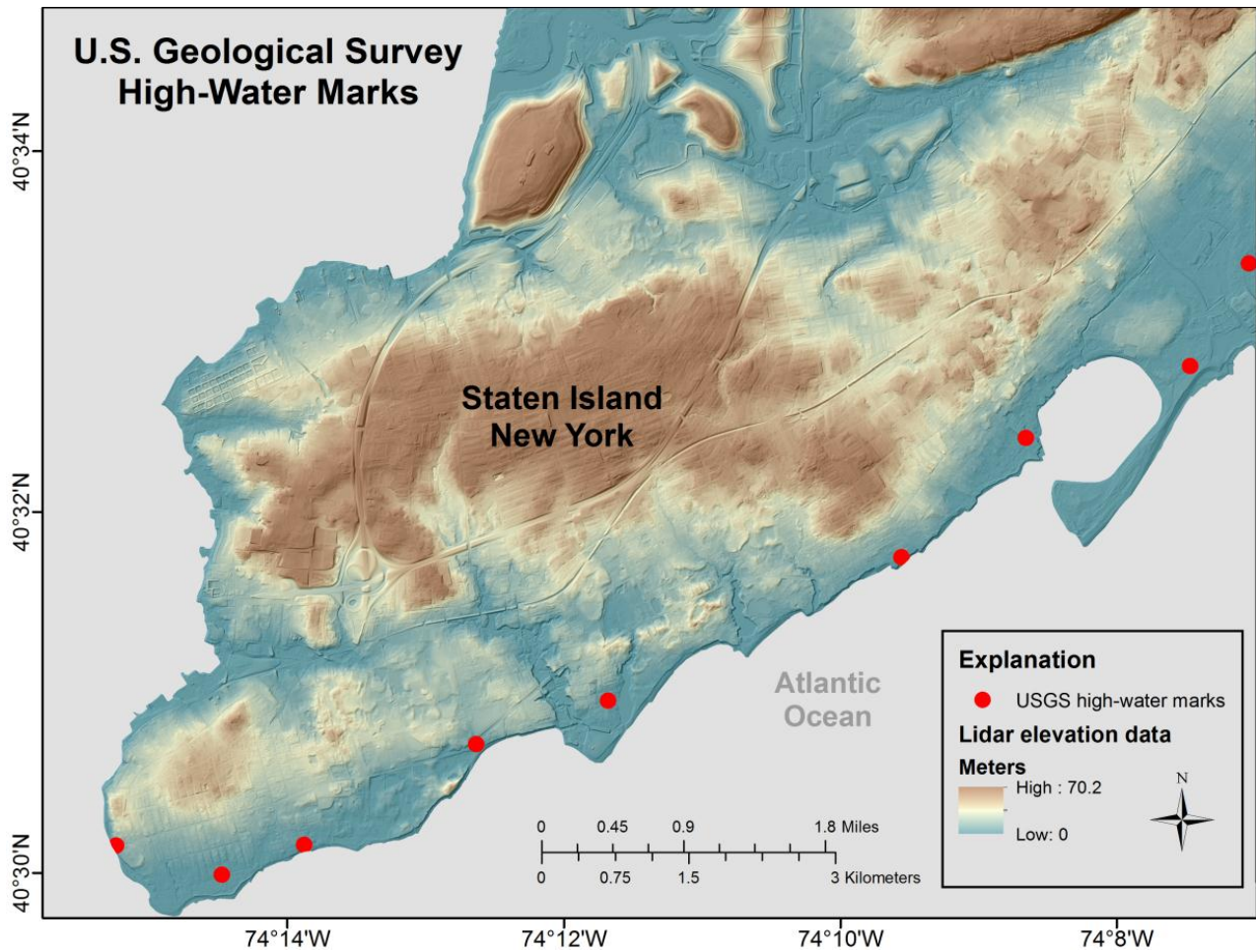


Figure 2. U.S. Geological Survey high-water marks collected in cooperation with the Federal Emergency Management Agency on the southern part of Staten Island, New York. We used the mean of GPS survey elevation values and high-water mark height above ground values to derive a single-value surface method inundation value. Also, see Table 1.

Table 1. Mean of U.S. Geological Survey GPS ground survey elevations and high-water marks in the study area. Also, see Figure 2.

Ground Surface Elevation (m)	High-Water Mark Height above Ground Surface Elevation (m)	Ground Surface Elevation and High-Water Mark Elevation (m)
3.99	0	3.99
4.02	1.69	5.71
4.02	0	4.02
3.96	0	3.96
2.99	0	2.99
3.99	0.29	4.28
5.15	0	5.15
4.27	0	4.27
3.81	2.40	6.21
--	Mean	4.51

The (4.51 m) inundation delineation was overlain on a shaded relief image of the study area lidar elevation surface (1 m). We visually compared the inundation delineation with the shaded relief to identify inland areas that were not hydrologically connected to the ocean because of raised features such as bridges or elevations representing road features. We also calculated the surface area of our inundation delineation (4.51 m) to compare with a FEMA Modeling Task Force (MOTF)-Hurricane Sandy Impact Analysis storm surge boundary [29].

FEMA MOTF utilized USGS HWMs [27,28] and storm surge sensor data [30] to interpolate a 1 m resolution water surface elevation that was subtracted from the best available DEM to create a depth grid and surge boundary by State [29]. We downloaded the FEMA MOTF water surface elevation (grid) (NAVD88 in units of meters) and the storm surge boundary (vector) [29] to calculate the surface area. In ArcGIS, we overlaid the (4.51 m) inundation delineation that we generated with the FEMA MOTF storm surge (vector) boundary to visually compare the differences between the two delineations. We assessed the overlay analysis to identify hydrologically disconnected inland areas.

4. Results and Discussion

4.1. Hydrologically Disconnected Inland Areas

In the study area where lidar elevation values were raised by 4.51 m (Table 1), there were several inland areas that were hydrologically disconnected from the Atlantic Ocean, particularly upstream of raised features, such as bridge decks or elevations overlaying constructed culvert drainage structures. Figure 3 shows an example location of the inundation delineation (blue) that we generated in the study area. Notice the three inland areas in the red circles that are disconnected from downstream waters. In an elevation-derived surface flow model, these areas lack hydrologic connectivity because the roads (raised features in the lidar elevation surface) prevent continuous flow across the lidar elevation surface. The road elevation values are greater than the specified inundation value of 4.51 m; therefore the roads are not considered inundated in this example, even though the bare earth surface under bridges or culvert drainage structures under road surfaces could act as a conduit given a flood or storm surge scenario. Unless the lidar elevation surface is hydrologically-enforced [9,10,13] to enable hydrologic models to simulate flow under bridges and through culverts, this issue can cause problems for an inundation analysis.

For validation purposes, we compared the (4.51 m) inundation delineation shown in Figure 3 with the FEMA MOTF-Hurricane Sandy Impact Analysis storm surge boundary [29] shown in Figure 4. Both delineations show similarities, however the inland areas that are inundated in the red circles in Figure 3 are not included in the FEMA MOTF storm surge boundary in Figure 4. It should be noted that our focus was not to replicate what FEMA MOTF published for a storm surge boundary [29] or to show any underestimation of water surface height by FEMA, but rather to identify inland areas that are potentially subject to inundation yet are disconnected from ocean waters due to raised (road) features in the lidar elevation surface. Regardless of the technique, notice that both Figures 3 and 4 show that road elevations overlaying drainage structures prevent hydrologic connectivity from inland areas to ocean waters. In the lidar elevation surface, these types of elevated (road) features can be identified and hydrologically-enforced [9,10,12,13] to consider inland areas prior to inundation analysis.

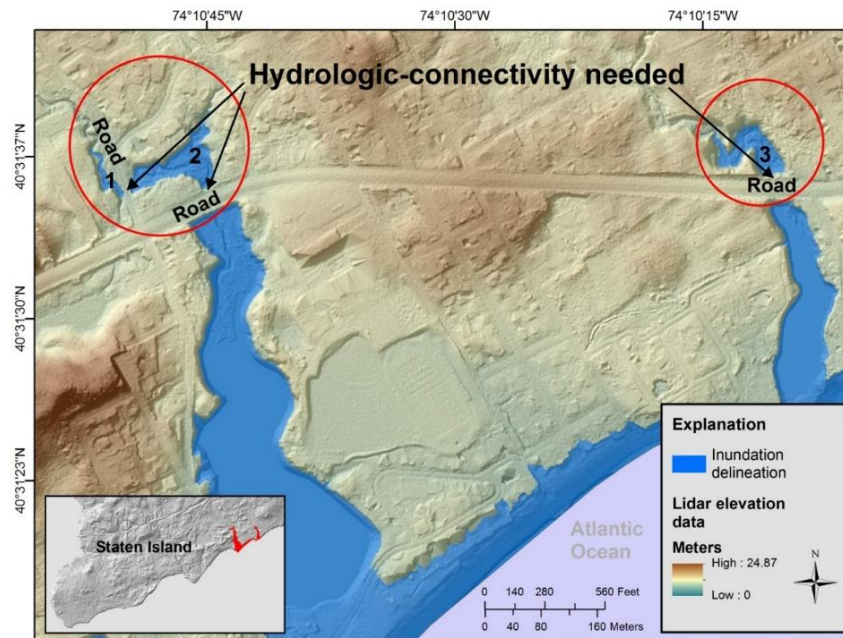


Figure 3. Inundation delineation (blue) that represents lidar elevation values lower than 4.51 m overlain on a high-resolution lidar elevation shaded relief. The roads inside the red circles should be hydrologically-enforced to achieve hydrologic connectivity between the inland inundated areas and the Atlantic Ocean so the inland areas can be considered for an inundation analysis. This is what the coastal inundation would look like if the roads were hydrologically-enforced.

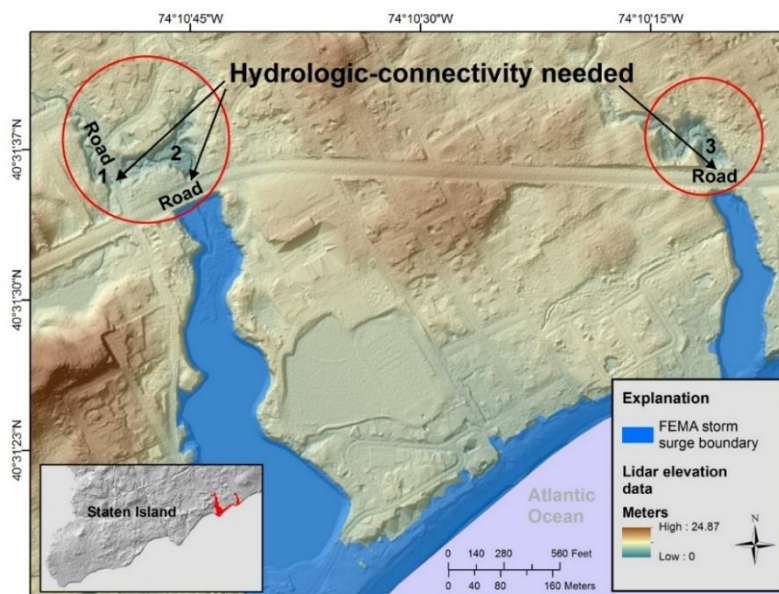


Figure 4. Federal Emergency Management Agency (FEMA) Modeling Task Force (MOTF)-Hurricane Sandy Impact Analysis storm surge boundary. The boundary is overlain on a high-resolution lidar elevation shaded relief. Inland areas that are inundated in Figure 3 (red circles) are not included in the FEMA MOTF storm surge boundary shown in this figure. This is what the coastal inundation would look like if the roads were not hydrologically-enforced.

Figures 3 and 4 are just a few examples shown at a fine scale to illustrate the need for hydrologic connectivity between inland and ocean waters. We also found similar inland areas throughout the study area that needed hydrologic connectivity as well. These locations are shown in Figure 5 (red circles) along with a spatial comparison of the (4.51 m) inundation delineation (yellow) and the FEMA MOTF storm surge boundary (blue) overlain on a lidar elevation shaded relief.

Although both inundation delineations are comparable in Figure 5, we found that several inland areas were in need of hydrologic connectivity where there was a low variability of the USGS HWMs. For example, in Figure 5, at the top right, notice that the HWM (red point) measured 6.21 m while just southwest of that location the lowest HWM measured 2.99 m. This high (3.22 m) variability is to be expected, particularly with an intense storm event where local areas are impacted differently depending upon the storm surge and topography. Notice in this area of high variability that we did not identify any inland areas that lacked hydrologic connectivity. However, in locations where there was less HWM variability (< 1.2 m), we identified several inland areas in need of hydrologic connectivity (Figure 5, between HWM measurements of 4.29 m and 5.15 m).

We initially decided to use the nine available USGS HWM measurements in the study area to derive a mean inundation value of 4.51 m. That decision was made prior to any research results. Had we known that most of the inland areas in the central part of the study area needed hydrologic connectivity, we may have considered using just the three HWMs near that area. However, the mean inundation value would have differed by only 0.04 m and most likely would not have shown any different results.

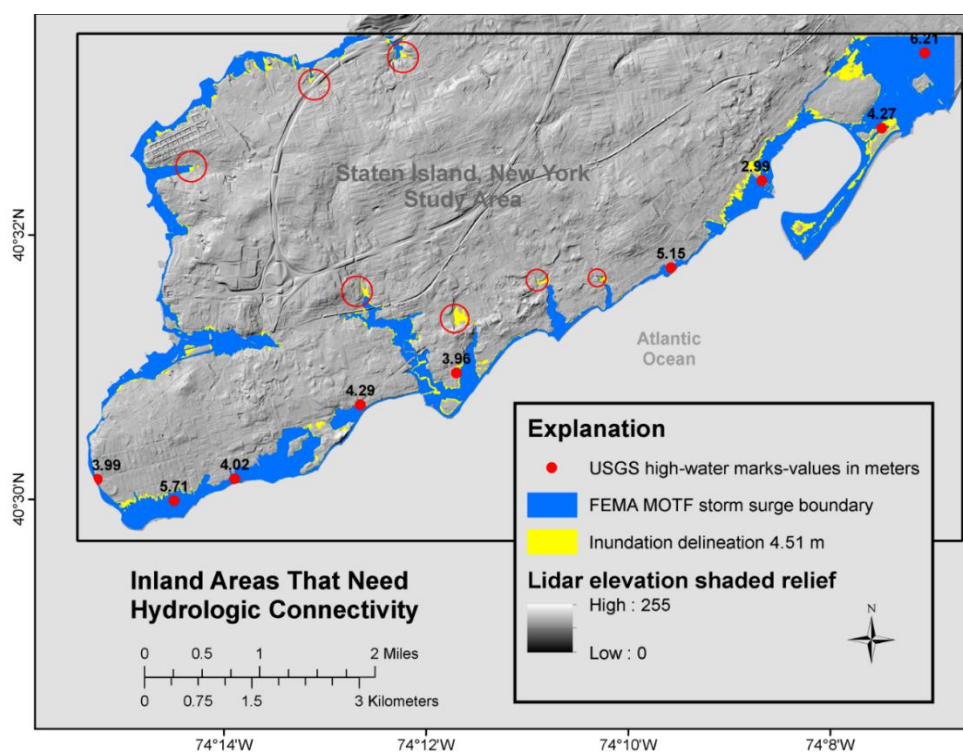


Figure 5. Comparison of the (4.51 m) inundation delineation (yellow) and the FEMA MOTF storm surge boundary (blue) overlain on a lidar elevation shaded relief. USGS high-water marks measurements (red points) are shown along with inland areas in need of hydrologic connectivity (red circles).

The calculated area of the inland locations shown in Figure 5 (red circles) exceeded 11 ha (~0.11 km²). Most of these locations were near the southern shore of Staten Island, New York, and thus would need hydrologic connectivity to the Atlantic Ocean. If bridge decks and road elevations overlying culverts were hydrologically-enforced in the lidar elevation surface (Figures 3 and 4), the 11 ha (~0.11 km²) could be considered in inundation delineations. For example, hydro-enforcement of lidar elevation surfaces enables hydrologic models to simulate flow under bridges and through culverts [13] in locations where water would flood in a given event. Therefore, preparing a lidar elevation surface as a hydrologic surface by hydrologically-enforcing drainage structures locations [9,10,13] may enhance the delineation of storm surge boundaries, especially in locations where the elevation surfaces have not been modified to represent the bare-earth surface. Therefore, lidar-derived hydrologic surfaces that take into account constructed drainage structures (culverts/bridges) are needed for hydrodynamic modeling [12,13,31].

The study area in this article is densely vegetated with urban areas interspersed as shown in Figure 6, which displays a 2013 high-resolution (1 m) aerial photograph obtained from the U.S. Department of Agriculture National Agriculture Imagery Program [32]. This is the same geographic location as shown in Figures 3 and 4. Notice in Figure 6 that the inland areas in need of hydrologic connectivity (red circles) are vegetated and it is difficult to see any stream channels, bridges, or culverts. In comparison, the stream channels in the inland areas show up clearly in the lidar elevation surface, and it is visually evident that overland flow drains into the Atlantic Ocean (Figures 3 and 4).

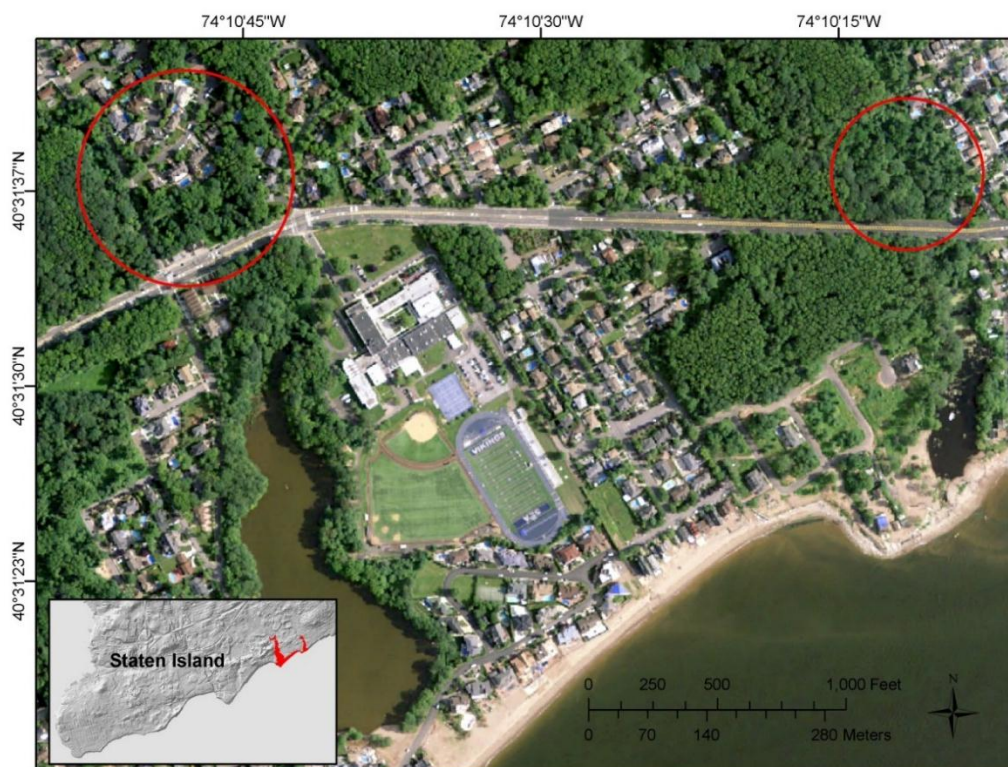


Figure 6. Aerial photograph of the same location shown in Figures 3 and 4. The inland areas in need of hydrologic connectivity (red circles) are located in a densely vegetated area. The 2013 imagery was obtained from the U.S. Department of Agriculture, National Agriculture Imagery Program.

4.2. Types of Physical Surfaces Potentially Impacted

Several locations in need of hydrologic connectivity were near large water bodies; therefore, we calculated the type of land cover for each inland area in the study area to determine what type of physical surfaces would potentially be impacted should the inland areas be considered as part of an inundation analysis. This was accomplished with an overlay analysis of the National Oceanic and Atmospheric Administration (NOAA), Office for Coastal Management, Coastal Change Analysis Program (C-CAP) Regional Land Cover data [33] and the (4.51 m) inundation delineation that we generated. The results are shown in Table 2. Low intensity developed land cover would be impacted the most at 0.03 km², followed closely by palustrine forested wetlands.

Table 2. National Oceanic and Atmospheric Administration, Office for Coastal Management, Coastal Change Analysis Program (C-CAP) Regional Land Cover data for inland areas in the study area.

National Oceanic and Atmospheric Administration Coastal Change Analysis Program (C-CAP) Regional Land Cover Classification	Area (km ²)
Developed, Low Intensity	0.0297
Palustrine Forested Wetland	0.0198
Developed, Medium Intensity	0.0171
Deciduous Forest	0.0171
Developed Open Space	0.0144
Open Water	0.0081
Palustrine Emergent Wetland	0.0063
Palustrine Scrub/Shrub Wetland	0.0009
Total	0.1134

The NOAA C-CAP land cover data were available at a 30 m resolution for the State of New York [33], whereas the inland areas, as shown in Figure 5, were derived from the high-resolution (1 m) lidar elevation surface [25]. Because of the differing resolution, two inland areas (< 30 m²) became excluded when the NOAA C-CAP data were extracted in the overlay analysis. The calculations for those areas are not included in Table 2; however, a visual analysis indicated that developed, medium intensity and palustrine forested wetland land cover types would be impacted in those locations. Perhaps a comparison of high-resolution land cover data (not currently available in the study area) with the (4.51 m) inundation delineation would improve upon this analysis.

We assessed the inland areas shown in Figures 3 and 4 (red circles) with photographs obtained by scientists from the College of Staten Island, The City University of New York [34]. These scientists also provided information about the drainage structures from a New York City Department of Environmental Protection (NYCDEP), Environmental Impact Statement (EIS) [35]. According to the NYCDEP EIS, location 1 is a brick arch structure with a concrete pipe (Figure 7). Location 2 is an 8 ft × 6 ft box culvert as shown in Figure 8. The photograph for location 3 shows no evidence of a culvert (Figure 9). However, there is a stagnant lake nearby and the culvert may be covered up with vegetation. Additionally, according to the NYCDEP EIS [35], there should be a twin box culvert than can handle 200 cfs at this location. In comparison,

notice that the lidar elevation surface shows evidence of river channels upstream and downstream of the roads in all three locations, thereby inferring hydrologic connectivity (Figures 3 and 4).



Figure 7. Photograph of inland area #1 (Figures 3 and 4). Photograph taken on 6 June 2015 by Michael Kress and Alan Benimoff College of Staten Island, The City University of New York.



Figure 8. Photograph of inland area #2 (Figures 3 and 4). Photograph taken on 6 June 2015 by Michael Kress and Alan Benimoff, College of Staten Island, The City University of New York.



Figure 9. Photograph of inland area #3 (Figures 3 and 4). Photograph taken on 6 June 2015 by Michael Kress and Alan Benimoff, College of Staten Island, The City University of New York.

An additional important variable to consider when delineating inundation is the accuracy of the lidar point cloud classifications. Lidar points classified as ground are used to generate a lidar bare earth elevation surface. Thus, inundation delineations are not only dependent upon the lidar elevation surface but also upon the accuracy of the lidar point classifications. As noted by Mason *et al.* [36], the basic problem in lidar (point cloud) post-processing is the classification of ground *versus* vegetation or buildings. Also, as defined in the USGS Lidar Base Specifications version 1.2 [37], the bare earth elevation surface is digital elevation data of the terrain, free from vegetation, buildings, and other man-made structures; in other words, elevations of the ground. Therefore, because this coastal study area contains numerous tidal wetlands and bogs, it can be challenging to classify the ground surface beneath the dense vegetation. If lidar points that represent vegetation are inadvertently classified as ground, a resulting bare earth surface may not be generated correctly, thereby impacting the modeling of overland surface flow based on the DEM.

5. Conclusions

Remotely sensed airborne lidar data are frequently used to generate high-resolution, high-vertical accuracy elevation surfaces that are critical for coastal area flood inundation delineations, flood monitoring and mapping, and flood management [4–7,38,39]. The detailed topographic information in a lidar elevation surface is critical to understanding the highly dynamic and populated coastal areas that are impacted by storm surge and inundation. Thus, lidar elevation surfaces are used to monitor and model coastal surface processes to delineate spatial inundation patterns.

Although a single-value surface method is often used to inundate lidar elevation surfaces that are below a specified elevation value, the approach does not take into consideration hydrologic connectivity and the flow of water across the landscape [8,20,22]. In the simplest case, without any water level inaccuracies included, the inundation from a single-value water surface model is dependent only on the elevation uncertainty [22]. Due to this uncertainty, we propagated a lidar elevation surface in a coastal region subject to flooding to demonstrate how bridge decks or elevations overlying culverts prevent hydrologic connectivity from inland areas to ocean waters [12,13,31]. Although the process of achieving hydrologic connectivity using hydro-enforcement methods is not new [9,10,12,13,18], the application of hydro-enforced lidar elevation surfaces for improved coastal inundation mapping as approached in this research is innovative. Hydrologically-connected lidar elevation surfaces are not always considered in hydrologic analyses. We demonstrated that an area exceeding 11 ha (~0.11 km²) could be included in inundation analysis to include upstream areas subject to flooding in a storm surge or hurricane event.

The purpose of this article is to improve upon inundation analyses and enhance hydrodynamic models that inundate high-resolution lidar elevation surfaces by accounting for hydrologic connectivity of inland areas with ocean waters. This information is needed for flood monitoring and management in sensitive coastal regions. Considering the hazardous effects of climate change events that impact sensitive coastal regions with hurricanes, storm surge, and inundation of homes and business in populated areas, inundation analysis is critically important for providing coastal tools and services to federal, state, local, and educational institutions. This information is needed to monitor and predict coastal hazard, inundation and storm surge prediction and analysis, and ecological impacts to coastal areas subject to such events.

Acknowledgments

The authors would like to thank Dean Gesch for reviewing this manuscript. His scientific expertise is greatly appreciated. We would also like to thank the anonymous journal reviewers for their thoughtful comments and suggestions. We are also grateful to Michael Kress and Alan Benimoff, College of Staten Island, The City University of New York, for graciously providing photographs and information about some of the drainage structures in the study area. We are very thankful for their willingness to assist us. Their scientific expertise of Staten Island's vulnerability to storm surge is well published. We also want to express our sincere appreciation for Cindy Thatcher's assistance in obtaining the photographs. Any use of trade, firm, or product names is for descriptive purposes only and does not imply endorsement by the U.S. Government.

Author Contributions

Sandra Poppenga and Bruce Worstell analyzed the data and prepared the manuscript.

Conflicts of Interest

The authors declare no conflict of interest.

References

1. Burkett, V.R.; Davidson, M.A. *Coastal Impacts, Adaptation and Vulnerability: A Technical Input to the 2013 National Climate Assessment*; Island Press: Washington, DC, USA, 2012.
2. Buxton, H.T.; Andersen, M.E.; Focazio, M.J.; Haines, J.W.; Hainly, R.A.; Hippe, D.J.; Sugarbaker, L.J. *Meeting the Science Needs of the Nation in the Wake of Hurricane Sandy—A U.S. Geological Survey Science Plan for Support of Restoration and Recovery*; U.S. Geological Survey Circular 1390; US Geological Survey: Reston, VA, USA, 2013.
3. Brock, J.C.; Purkis, S.J. The emerging role of LiDAR remote sensing in coastal research and resource management. *J. Coast. Res.* **2009**, doi:<http://dx.doi.org/10.2112/SI53-001.1>.
4. Gesch, D.B. Analysis of lidar elevation data for improved identification and delineation of lands vulnerable to sea level rise. *J. Coast. Res.* **2009**, doi:<http://dx.doi.org/10.2112/SI53-006.1>.
5. Gesch, D.B.; Guiterezz, B.T.; Gill, S.K. Coastal elevations. In *Coastal Sensitivity to Sea Level Rise: A Focus on the Mid-Atlantic Region*; Titus, J.G., Anderson, K.E., Eds.; U.S. Climate Change Science Program: Washington, DC, USA, 2009; pp. 25–42.
6. Benimoff, A.I.; Fritz, W.J.; Kress, M. Superstorm Sandy and Staten Island: Learning from the past, preparing for the future. In *Learning from the Impacts of Superstorm Sandy*; Bennington, J.B., Farmer, E.C., Eds.; Elsevier Inc.: New York, NY, USA, 2015; pp. 21–40.
7. Brock, J.; Sallenger, A.H. *Airborne Topographic Lidar Mapping for Coastal Science and Resource Management*; U.S. Geological Survey Open File Report 2001–46; US Geological Survey: Reston, VA, USA, 2001.
8. Gesch, D.B. Consideration of vertical uncertainty in elevation-based sea-level rise assessments: Mobile Bay, Alabama case study. *J. Coast. Res.* **2013**, doi:<http://dx.doi.org/10.2112/SI63-016.1>.
9. Poppenga, S.K.; Worstell, B.B.; Stoker, J.M.; Greenlee, S.K. *Using Selective Drainage Methods to Extract Continuous Surface Flow from 1-meter Lidar--Derived Digital Elevation Data*; U.S. Geological Survey Scientific Investigations Report 2010–5059; US Geological Survey: Reston, VA, USA, 2010.
10. Poppenga, S.K.; Worstell, B.B.; Stoker, J.M.; Greenlee, S.K. Using selective drainage methods to hydrologically-condition and hydrologically-enforce lidar-derived surface flow. In *Proceedings of the Remote sensing and hydrology Symposium, Jackson Hole, WY, USA, 27–30 September 2010*; pp. 329–332.
11. FEMA. Guidelines and Standards for Flood Risk Analysis and Mapping. Available online: <http://www.fema.gov/guidelines-and-standards-flood-risk-analysis-and-mapping> (accessed on 10 February 2015).
12. Poppenga, S.K.; Worstell, B.B. Hydrologic connectivity: A quantitative assessment of hydrologic-enforced drainage structures in an elevation model. *J. Coast. Res.* **2015**, in press.
13. Poppenga, S.K.; Worstell, B.B.; Danielson, J.J.; Brock, J.C.; Evans, G.A.; Heidemann, H.K. *Hydrologic Enforcement of Lidar DEMs*; U.S. Geological Survey Fact Sheet 2014–3051; US Geological Survey: Reston, VA, USA, 2014.
14. ARCADIS U.S. Inc. *ADCIRC Based Storm Surge Analysis of Sea Level Rise in Grand Bay*; The Nature Conservancy: Arlington, VA, USA, 2011.

15. MacDonald, T. Vulnerability and impacts on human development. In *Coastal Impacts, Adaptation, and Vulnerabilities: A Technical Input to the 2013 National Climate Assessment*; Burkett, V.R., Davidson, M.A., Eds.; NOAA: Washington, DC, USA, 2012; pp. 66–97.
16. Karlin, A.; McClung, G.; Janke, J. Flood-prone area mapping: A case study. In *Manual of Airborne Topographic Lidar*; Renslow, M.S., Ed.; American Society for Photogrammetry and Remote Sensing: Bethesda, MD, USA, 2012; pp. 345–352.
17. Kress, M.E.; Benimoff, A.I.; Fritz, W.J.; Thatcher, C.; Blanton, B.O.; Dzedzits, E. Modeling and simulation of storm surge on Staten Island to understand inundation analysis. *J. Coast. Res.* **2015**, in review.
18. Diaz-Nieto, J.; Lerner, D.N.; Saul, A.J.; Blanksby, J. GIS water-balance approach to support surface water flood-risk management. *J. Hydrol. Eng.* **2012**, *17*, 55–67.
19. Abdullah, A.F.; Vojinovic, Z.; Price, R.K.; Aziz, N.A.A. Improved methodology for processing raw LiDAR data to support urban flood modelling—accounting for elevated roads and bridges. *J. Hydroinf.* **2012**, *14*, 253–269.
20. Poulter, B.; Halpin, P.N. Raster modeling of coastal flooding from sea-level rise. *Int. J. Geogr. Inf. Sci.* **2008**, *22*, 167–182.
21. Gilmer, B.; Ferdana, Z. Developing a framework for assessing coastal vulnerability to sea level rise in southern New England, USA. In *Resilient Cities 2: Cities and Adaptation to Climate Change—Proceedings of the Global Forum 2011*; Otto-Zimmermann, K., Ed.; Springer: Dordrecht, The Netherlands, 2012; pp. 25–36.
22. National Oceanic and Atmospheric Administration Coastal Services Center. Mapping Inundation Uncertainty. Available online: http://coast.noaa.gov/digitalcoast/_pdf/ElevationMappingConfidence.pdf (accessed on 2 June 2015).
23. U.S. Geological Survey. Hurricane Sandy. Available online: <http://www.usgs.gov/hurricane/sandy/> (accessed on 12 May 2015).
24. New York City Office of Emergency Management. NYC Hazards: NYC Hurricane History. Available online: http://www.nyc.gov/html/oem/html/hazards/storms_hurricanehistory.shtml (accessed on 20 May 2015).
25. Woolpert. Lidar Point Cloud Data and Digital Elevation Model for Richmond County, New York. Available online: <http://earthexplorer.usgs.gov/> (accessed on 10 February 2015).
26. Woolpert. *Airborne Lidar Task Order Report, New York CMGP Sandy 0.7 m NPS Lidar*; Woolpert Project Number 73666; US Geological Survey: Rolla, MO, USA, 2014.
27. McCallum, B.E.; Wicklein, S.M.; Reiser, R.G.; Busciolano, R.; Morrison, J.; Verdi, R.J.; Painter, J.A.; Frantz, E.R.; Gotvald, A.J. *Monitoring Storm Tide and Flooding from Hurricane Sandy along the Atlantic Coast of the United States, October 2012*; US Geological Survey Open-File Report 2013–1043; U.S. Geological Survey: Reston, VA, USA, 2013.
28. U.S. Geological Survey. Sandy Mapper Database. Available online: <http://water.usgs.gov/floods/events/2012/sandy/sandymapper.html> (accessed on 11 March 2015).
29. FEMA-MOTF. FEMA MOTF Hurricane Sandy Impact Analysis. Available online: <http://www.arcgis.com/home/item.html?id=307dd522499d4a44a33d7296a5da5ea0> (accessed on 21 April 2015).

30. U.S. Geological Survey. Storm Surge Sensors. Available online: http://www.usgs.gov/blogs/features/usgs_science_pick/usgs-storm-surge-sensors/ (accessed on 21 April 2015).
31. Heidemann, H.K. Digital elevation models. In *Manual of Airborne Topographic Lidar*; Renslow, M.S., Ed.; American Society for Photogrammetry and Remote Sensing: Bethesda, MD, USA, 2012; pp. 283–310.
32. U.S. Department of Agriculture, Natural Resources Conservation Service, Geospatial Data Gateway. Available online: <https://gdg.sc.egov.usda.gov/> (accessed on 6 August 2015).
33. National Oceanic and Atmospheric Administration, C-CAP FTP Download. Available online: <http://coast.noaa.gov/ccapftp/> (accessed on 4 June 2015).
34. Kress, M.; Benimoff, A. (College of Staten Island, The City University of New York, Staten Island, New York, USA). Photographs of inland areas, 2015.
35. New York City Department of Environmental Protection. *Blue Heron, Arbutus Creek, and Lemon Creek/Sandy Brook Watershed Drainage Plans, Final Environmental Impact Statement*; CEQR No. 97DEP026; City of New York: New York, NY, USA, 1998.
36. Mason, D.C.; Horritt, M.S.; Hunter, N.M.; Bates, P.D. Use of fused airborne scanning laser altimetry and digital map data for urban flood modelling. *Hydrol. Process.* **2007**, *21*, 1436–1447.
37. Heidemann, H.K. *Lidar Base Specification (version 1.2, November 2014)*; U.S. Geological Survey: Reston, VA, USA, 2014.
38. Webster, T.L. Flood risk mapping using LiDAR for Annapolis Royal, Nova Scotia, Canada. *Remote Sens.* **2010**, *2*, 2060–2082.
39. Webster, T.L.; Forbes, D.L.; Dickie, S.; Shreenan, R. Using topographic LiDAR to map flood risk from storm surge events for Charlottetown, Prince Edward Island, Canada. *Can. J. Remote Sens.* **2004**, *30*, 54–76.

© 2015 by the authors; licensee MDPI, Basel, Switzerland. This article is an open access article distributed under the terms and conditions of the Creative Commons Attribution license (<http://creativecommons.org/licenses/by/4.0/>).